Using Polarization Analyzed SANS To Investigate the Effect Of Anisotropy On Magnetic Nanoparticle Interaction

1. Introduction

Magnetic nanoparticles and nanoscale structures are intriguing in part because of the exotic properties that can emerge compared with bulk. A reduction of magnetic moment per atom in magnetite (Fe_3O_4) with decreasing nanoparticle size, for example, is known to occur. This decrease in magnetism has been hypothesized to originate from surface disordering or anisotropy-induced radial canting [1-9], resulting in proposed morphologies that are difficult to verify using conventional magnetometry. Interestingly, recent experiments [10-12] suggest that in certain circumstances oleic acid coating may preserve the surface magnetism. When the nanoparticles are brought close together, additional dipolar interactions come into play.

Application of Polarization Analyzed Small-Angle Neutron Scattering (PASANS) to 9 nm magnetite nanoparticles closed-packed into face-centered crystallites of up to a micron revealed that at nominal saturation the missing magnetic moments unexpectedly interacted to form ordered shells 1.0 to 1.5 nm thick with a magnetic component canted perpendicular to their ferromagnetic cores between 160 to 320 K [13]. These shells additionally displayed intra-particle "cross-talk", *i.e.* they selected a common orientation over clusters of tens of nanoparticles (averaging to zero across the entire sample). However, the shells disappeared when the external field was removed and inter-particle magnetic interactions were negligible (at 300 K), confirming their magnetic origin. The canted shell response is thought to occur as the result of competition between Zeeman, dipolar, and exchange interactions.

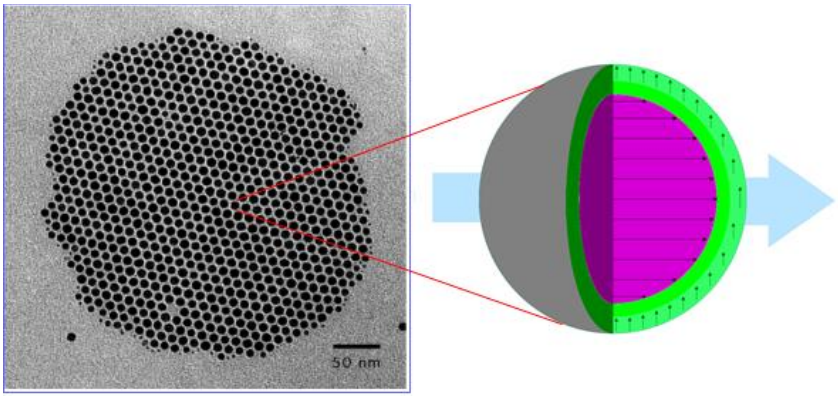

Figure 1 depicts a simplified schematic showing the uniformly canted magnetic shell (green area) with a component that is perpendicular to the applied field of 1.2 Tesla (shown as a light blue arrow).

In order to better understand the role of anisotropy, we shall study a similar system of close packed 9 nm spherical particles, but composed of cobalt ferrite ($CoFe_2O_4$) with an internal anisotropy (tendency for the magnetic spins to align along a particular crystalline axis) that is more than an order of magnitude higher. Using PASANS we will be able to:

1) Unambiguously separate the structural scattering from the magnetic scattering
2) Separate the magnetic scattering into components that are "parallel to" and "perpendicular to" an external applied field
3) Map how the magnetic scattering length densities vary as a function of field and temperature

4) Model the structural and magnetic scattering to see how anisotropy affect canted shell formation

2. Why Use SANS?

Small-angle x-ray scattering (SAXS) and small-angle neutron scattering (SANS) provide similar information regarding the macroscopic measurement of scattering cross-section, $d\Sigma / d\Omega(q)$. Yet, neutron scattering distinguishes itself in several ways: 1) strong hydrogen scattering cross-section, 2) sensitivity to hydrogen-deuterium substitution, 3) ability to contrast match many samples to solution based on hydrogen-deuterium content, and 4) sensitivity to magnetism. The former properties make neutrons ideal for study of many biological and polymer systems; the latter makes neutrons ideal for studying magnetic systems. Additionally, the manner in which the neutron spin processes upon scattering (to be discussed) allows both the magnitude and *orientation* of sample magnetic moments to be precisely determined.

3. The SANS Instrument

The SANS instrument NG7 is able to cover a q-range of 0.01 nm^{-1} to 7 nm^{-1}, which translates to features sizes below 1 nm and up to 500 nm. Recall that q (sometimes denoted Q) = $2\pi \sin(\alpha) / \lambda \approx 2\pi$/distance, where α is the scattering angle on the detector with respect to the unscattered neutron beam center. The neutron wavelength (λ) may be tuned between 0.5 nm and 2 nm with a wavelength spread between 11% and 22% full-width half-maximum.

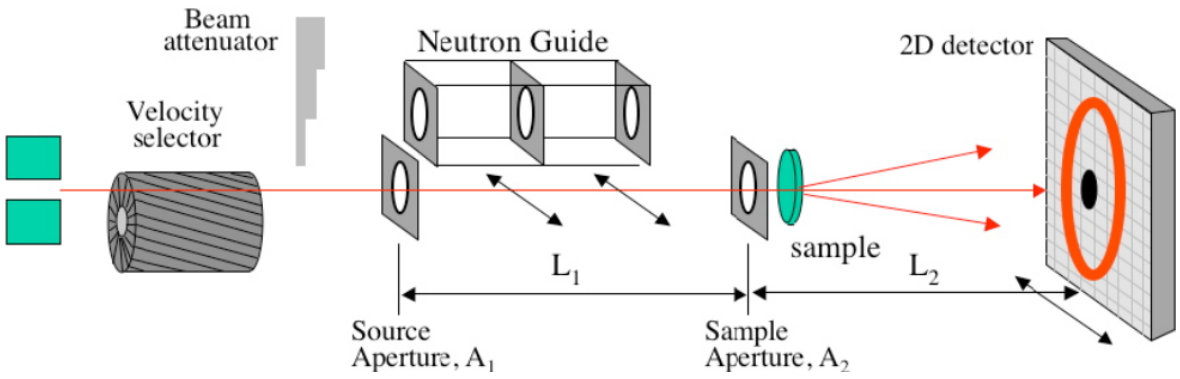

Figure 2 shows a schematic of the 30 meter SANS beamline at the NCNR without any of the polarized beam components.

In the case of a non-polarized (standard) beam experiment, the intensity of the scattering on the detector after background correction in the SANS experiment is given by

$$I_{meas} = \phi A d T (\frac{d\Sigma}{d\Omega}) \Delta\Omega \varepsilon t$$

where

ϕ is the number of neutrons per second per unit area incident on the sample

A is the sample area

d is the sample thickness

T is the sample transmission

$\Delta\Omega$ is the solid angle over which scattered neutrons are accepted by the analyzer

ε is the detector efficiency

t is the counting time

The aim of the SANS experiment is to obtain the differential macroscopic scattering cross-section dΣ/dΩ from I_{meas}. During a polarized scattering experiment, the efficiency of the polarizing components will additionally need to be corrected for (specialized SANS IGOR modules), but the fundamental aim remains.

4. Planning The Experiment

4a. Scattering Length Density

In order for there to be small-angle scattering, there must be scattering contrast, in this case between the nanoparticles, oleic acid coating, and air (≈ 0). The scattering is proportional to the scattering length density (abbreviated SLD or symbolized as ρ) *squared*. SLD is defined as

$$\rho = \frac{1}{V}\sum_{i}^{n} b_i$$

where V is the volume containing n atoms, and b_i is the (bound coherent) scattering length of the i^{th} atom in V. V is usually the molecular or molar volume for a homogeneous phase in the system of interest.

Neutrons are scattered either through interaction with the nucleus (nuclear scattering, N) or through interaction between the unpaired electrons (and hence the resultant magnetic moment, M) with the neutron spin. Hence, $CoFe_2O_4$ has both a nuclear SLD and a magnetic SLD and will display both nuclear and magnetic contrast.

Nuclear SLDs can be calculated from the above formula, using a table of the scattering lengths [14] for the elements, or calculated using the web based interactive SLD Calculator [15]. Magnetic SLD can be calculated using the following formula

$$\rho_m = M\left(in\ \frac{A}{m}\right) x\ 2.853\ x\ 10^{-6}\ \frac{m}{A\ \text{Å}^{-2}}$$

Some handy magnetic conversions are:

$$\frac{A}{M} = 1000\frac{emu}{cc};\ \mu_B = 9.274\ x\ 10^{-21}\ emu$$

The magnetic saturation of *bulk* $CoFe_2O_4$ (at 5 K) is 497.7 emu/cc [16]. Note that nanoparticles may vary from bulk due to dislocations and from the effect of surface termination sites. Table 1 provides some useful SLDs for our experiment.

Material (bulk)	Chemical Formula	SLD_nuclear ($Å^{-2}$)	SLD_magnetic ($Å^{-2}$)
Cobalt ferrite	$CoFe_2O_4$	6.07 x 10^{-6}	1.42 x 10^{-6}
Magnetite	Fe_3O_4	6.97 x 10^{-6}	1.46 x 10^{-6}
Oleic Acid	$C_{18}H_{34}O_2$	7.81 x 10^{-8}	0

Table 1. Nuclear and magnetic scattering length densities of interest

4b. Sample Thickness

Given the calculated sample contrast, how thick should the sample be? Recall that the scattered intensity is proportional to the product of the sample thickness, d_s, and the sample transmission, T. It can be shown that the transmission, which is the ratio of the transmitted to the incident beam intensity, is given by

$$T = e^{-\sum_t d_s}$$

where $\sum_t = \sum_c + \sum_i + \sum_a$ (the sum of the coherent, incoherent, and absorption macroscopic cross sections). The absorption cross section, $\sum_a$, can be accurately calculated from tabulated absorption cross sections of the elements (and isotopes) if the mass density and chemical composition of the sample are known. The incoherent cross section, $\sum_i$,can be estimated from the cross section tables for the elements as well, but not as accurately as it depends on the atomic motions and is, therefore, temperature dependent. The coherent cross section, $\sum_c$, can be estimated from the details of both the structure and the correlated motions of the atoms in the sample. This should be no surprise as $\sum_c$ as a function of angle is the quantity we are aiming to measure!

The scattered intensity is proportional to d_sT and hence

$$I_{meas} \propto d_s e^{-\sum_t d_s}$$

which has a maximum at $d_s = 1/\sum_t$ and implies an optimal transmission at 1/e = 0.37. The sample thickness at which this occurs is known as the "1/e" length.

The NCNR SLD calculator [15] provides estimates of 1/e length, which is about 4.5 mm for $CoFe_2O_4$. However, since our particles are not uniform , but rather have strong repeatable lattice spacing (strong Bragg scattering), we reduce the thickness to avoid multiple scattering.

4c. SASCALC

SASCALC is a tool built into the SANS IGOR reduction package that allows different beamline configurations to be simulated, helping users to select an ideal balance between desired q-range and maximum beam intensity. One such good configuration for this experiment would be:

```
Source Aperture Diameter =      5.00 cm
Source to Sample =               487 cm
Sample Aperture to Detector =    280 cm
Beam diameter =                 4.06 cm
Beamstop diameter =             2.00 inches
Minimum Q-value =             0.0154 1/Å (sigQ/Q = 23.9 %)
Maximum Horizontal Q-value =  0.1456 1/Å
Maximum Vertical Q-value =    0.1456 1/Å
Maximum Q-value =             0.2049 1/Å (sigQ/Q = 4.8 %)
Beam Intensity =          1307589 counts/s
Figure of Merit =            3.27e+07 Å^2/s
Attenuator transmission =     0.00122 = Atten # 8
***************** NG 3 *****************
Sample Aperture Diameter =          0.64 cm
Number of Guides =                  7
Sample Chamber to Detector =        220.0 cm
Sample Position is                  Huber
Detector Offset =                   0.0 cm
Neutron Wavelength =                5.00 Å
Wavelength Spread, FWHM =           0.109
Sample Aperture to Sample Position =5.00 cm
Lenses are OUT
```

If time permits, we may select and run an additional lower-q range (to survey longer spatial distances or correlations spanning multiple nanoparticles) together.

5. Magnetic SANS

5a. Magnetic Scattering

Small-angle neutron scattering is ideal for obtaining nuclear and magnetic structure, even for small magnetic moments that aren't necessarily all oriented in the same direction, with sub-nanometer resolution. Normally neutrons are unpolarized, meaning their spins points point

randomly in all directions. In the presence of a magnetic field (H), half the neutron spins will align with the field; half anti-parallel to the applied field. The first selection rule of neutron scattering is that only the component of a magnet moment oriented perpendicular to the scattering wave vector, q, participates in scattering. Thus, if an applied magnetic field (H) is set along X and the detector is in the X-Y plane, magnetic moments oriented along Y or Z (M_Y, M_Z) may be detected if measuring along the X-direction, while magnetic moments oriented along X or Z (M_X, M_Z) may be detected if measuring along the Y-direction (Figure 3). Note that an applied magnetic field required to align the neutron spins may be quite small (say 0.005 Tesla or less), which may not align the magnetic spins within the sample.

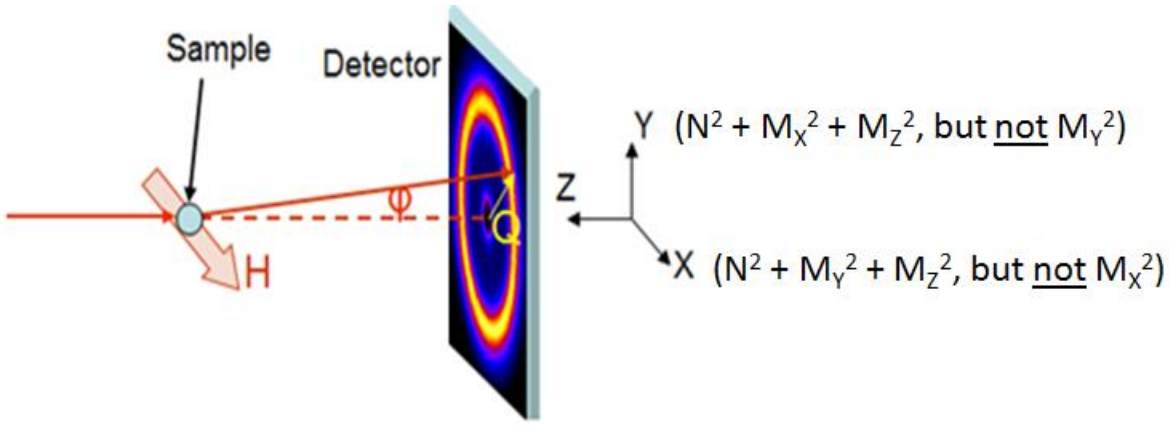

Figure 3. Unpolarized scattering with an applied magnetic field, H, set along the X-direction. Note how only the components of the sample magnetism perpendicular to q (noted on right hand side) may be seen in the scattered intensity.

Assuming that the nuclear scattering is isotropic, this gives a way to separate nuclear and magnet scattering contributions. The measured scattering intensity, I, is proportional to the squared sum of the spatial nuclear (N^2) and magnetic (M^2) Fourier transforms, defined as

$$N, M_J(q) = \sum_K \rho_{N,M_J}(K) e^{iq \cdot R_K}$$

where J is any Cartesian coordinate, $\rho_{N,M}$ is the nuclear or magnetic scattering length density, and R_K is the relative position of the K^{th} scatterer. Note that because we can only measure the absolute value of the Fourier Transform squared in a scattering experiment, rather than the complex components of the Fourier Transform itself, we lose *phase* information. The result is

that we may not be able to uniquely distinguish between a family of curves that model our data – a fact that should be kept in mind during data fitting and analysis.

Now, let us consider the case of Fe_3O_4 nanoparticles under the influence of a *saturating* magnetic field of 1.2 Tesla, such that the magnetic spins align along X (|| H). In this case, the X-axis contains only nuclear scattering, while the Y-axis contains nuclear scattering plus magnetic scattering from moments along X (M_X^2), as shown in the Figure 4.

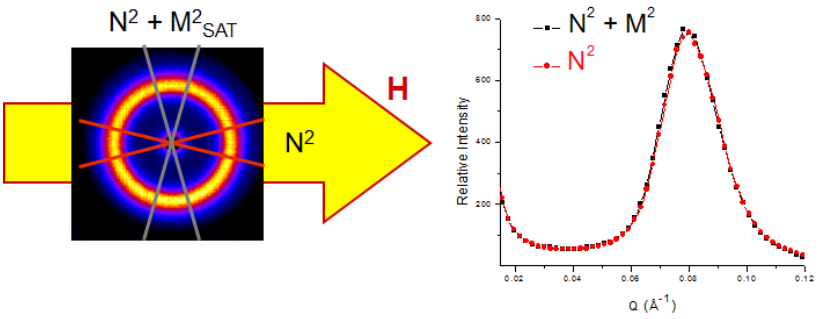

Figure 4. Comparison of horizontal and vertical sector cuts, with H || X, can be used to separate nuclear and magnetic scattering contributions if the structural scattering is isotropic. Scattering from a sample of Fe_3O_4 nanoparticles at 1.2 Tesla is shown.

In Figure 4, the diffraction peak comes from the fact that the nanoparticles are close-packed into μm-sized, ordered , face-centered cubic arrays with a prominent [111] diffraction peak centered at 0.08 $Å^{-2}$. The reason that the sector cuts along X and Y are so similar, although only the latter contains the magnetic scattering contribution, is that the ratio of magnetic to nuclear scattering, ρ^2_M / ρ^2_N is only 4% (refer to Table 1). For this reason, *polarization analyzed* SANS is useful to directly measure the magnetic scattering when the magnetic scattering contribution is small compared to the structural scattering contribution (demonstrated in section 5b. using the same Fe_3O_4 sample).

5b. Polarization Analysis

As discussed previously, an applied magnetic field realigns the spins of a neutron beam, normally randomly oriented, so that half of the spins become parallel with H, and the other half become anti-parallel to H. Now, one spin state can be preferentially selected over the other, using a polarizing element such an FeSi supermirror. The supermirror is a specially made magnetic diffraction grating that looks different to neutrons aligned parallel and anti-parallel to the applied field, thus scattering neutron spins of one orientation (for example up, denoted ↓) while allowing the spins of the other orientation (down, denoted ↑)to pass through. From here, the ↑ neutrons can be reversed at will using an electromagnetic flipper coil. After interaction with the sample, an analyzing glass cell filled with polarized ^{3}He preferentially allows

neutrons with spins aligned with the ^{3}He atoms to pass through, while absorbing neutrons with oppositely aligned spins (producing ^{4}He). This differs from the supermirror in that a divergently scattered beam, not just a tightly collimated one, may be surveyed at once. The ^{3}He orientation can be reversed at will with a nuclear magnetic resonance (NMR) pulse of an appropriate frequency. This combination, depicted in Figure 5, allows one to measure scattering cross-sections of ↑↑, ↓↑, ↓↓, and ↑↓ (where the first arrow indicate the spin before sample scattering and the second arrow indicates the neutron spin after sample scattering).

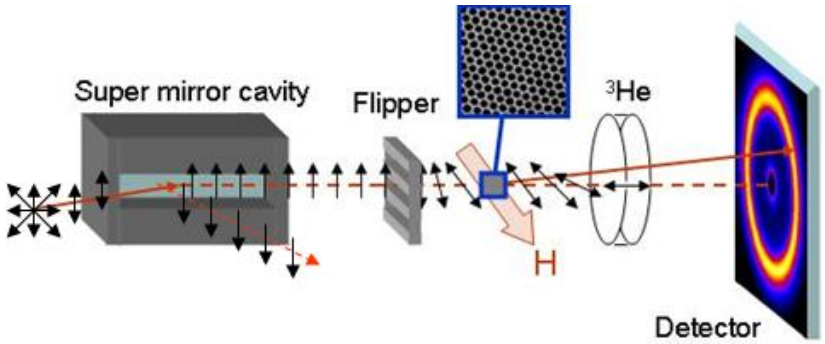

Figure 5. Polarization analysis set-up for a SANS instrument consists of a spin polarizing supermiror, a neutron spin flipper, a sample area with optional applied field, a spin analyzing ^{3}He cell, and a 2D detector.

As will be discussed in more detail, the ^{3}He polarization is time dependent. Yet, the polarization efficiency of each polarizing element can be measured with neutrons and corrected for within the SANS reduction framework. For any polarizing/analyzing element, the degree of polarization, P, is defined as the difference between the ↑ and ↓neutrons after passing through a polarizing device, divided by the total number of incoming neutrons (↑ + ↓):

$$P = \frac{\uparrow - \downarrow}{\uparrow + \downarrow}$$

The utility of adding polarization analysis for measuring M^2 is immediately obvious from Figure 6. Sector slices about the X-axis and Y-axis, resulting from the ↑↑ and ↓ ↓ scattering cross-sections, contain easily observable $\pm$NM cross-terms.

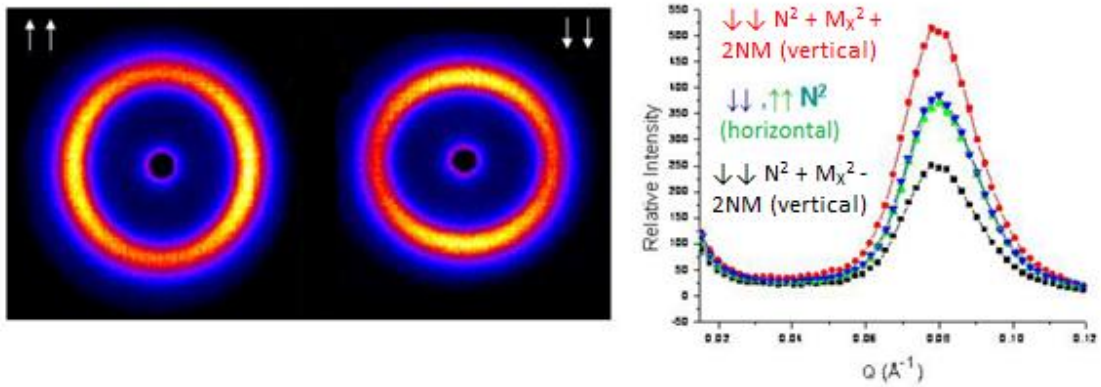

Figure 6. The net magnetism from a magnetically semi-saturated or saturated sample can be more readily observed using polarization analysis than using unpolarized neutrons (see Figure 4) when the nuclear scattering dominates the magnetic scattering. The sample shown consists of Fe_3O_4 nanoparticles in a field of 1.2 Tesla.

5c. Spin Selection Rules

The original rule (discussed for unpolarized neutrons) that only the component of M $\perp$ Q can participate in scattering also holds true for polarized neutrons. Additionally, of this projection of M $\perp$ Q, the part that is also || to the neutron polarization axis (defined by H) does not reverse the neutron spin. The remaining projection of M $\perp$ Q that is $\perp$ to the neutron polarization axis (defined by H) does reverse the neutron spin. These processes are denoted as non spin-flip (NSF) and spin-flip (SF) scattering, respectively. The nuclear scattering does not affect with the neutron spin, and so all structural scattering is confined to the NSF scattering. These rules are summarized in Figure 7.

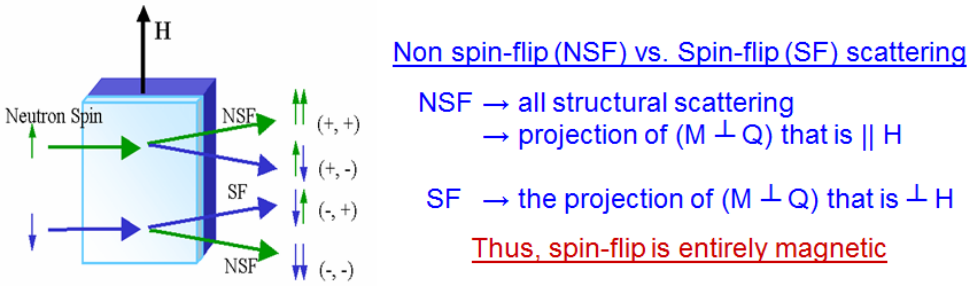

Figure 7. A summary of the nuclear and magnetic spin scattering selection rules.

The spin selection rules can be represented mathematically in terms of the Halpern-Johnson vector [17], which translates into the following equations [18-19] where H || X and θ is the angle between the positive X-axis and Q:

$$I^{\downarrow\downarrow,\uparrow\uparrow} = |N|^2 + sin^4(\theta)|M_X|^2 + \ sin^2(\theta)cos^2(\theta)|M_Y|^2 - [M_X{}^*M_Y + M_Y{}^*M_X]sin^3(\theta)cos^1(\theta)$$
$$\pm [M_X{}^*N + N^*M_X]sin^2(\theta) \ \mp [M_Y{}^*N + N^*M_Y]sin^1(\theta)cos^1(\theta)$$

$$I^{\uparrow\downarrow,\downarrow\uparrow} = |M_Z|^2 + cos^4(\theta)|M_Y|^2 + \ sin^2(\theta)cos^2(\theta)|M_X|^2$$
$$- [M_X{}^*M_Y + M_Y{}^*M_X]sin^1(\theta)cos^3(\theta) \ \pm i[M_Z{}^*M_X - M_X{}^*M_Z]sin^1(\theta)cos^1(\theta)$$
$$\mp i[M_Z{}^*M_Y - M_Y{}^*M_Z]cos^2(\theta)$$

Note that the equations simplify greatly along the X and Y axis. This is shown pictorially in Figure 8 using the Fe_3O_4 example data discussed previously.

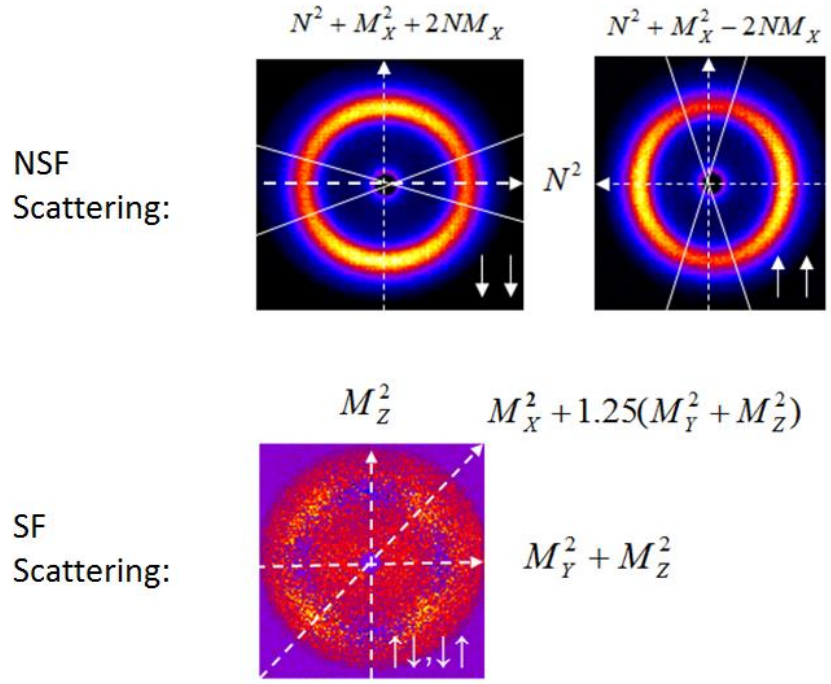

Figure 8. Simplification of the magnetic scattering equations occurs along the coordinate axes, as shown by the white arrows. Note the spin-flip scattering pattern is entirely magnetic, while the non spin-flip scattering contains the nuclear scattering contribution. The sample shown consists of Fe_3O_4 nanoparticles at 1.2 Tesla.

Thus, the following operations can be performed [18] to extract specific components of interest:

$$|N|^2 = I^{\uparrow\uparrow}(\theta = 0^o) = I^{\downarrow\downarrow}(\theta = 0^o)$$

$$|M_X|^2 = [I^{\downarrow\downarrow}(\theta = 90^o) + \ I^{\uparrow\uparrow}(\theta = 90^o)] - [I^{\downarrow\downarrow}(\theta = 0^o) + \ I^{\uparrow\uparrow}(\theta = 0^o)], assuming \ \ isotropic \ |N|^2$$

$$|Net\ M_X|^2 = \frac{[I^{\downarrow\downarrow}(\theta = 90^o) - I^{\uparrow\uparrow}(\theta = 90^o)]^2}{8|N|^2}, assuming\ \ isotropic\ |N|^2$$

$$|M_\perp|^2 = \frac{I^{\uparrow\downarrow}(\theta = 0^o) + I^{\downarrow\uparrow}(\theta = 0^o) + I^{\uparrow\downarrow}(\theta = 90^o) + I^{\downarrow\uparrow}(\theta = 90^o)}{3}, assuming\ \ |M_Y|^2 = |M_Z|^2$$

Let us now apply these operations once more to the Fe_3O_4 example system at 200 K in an applied magnetic field of 1.2 Tesla (|| X). The results are shown in Fig. 9 where sector slices of $\pm$ 10^o are taken about the X and Y axis to approximate θ = 0^o and 90^o degree scattering respectively. We can now clearly see that the nuclear Bragg peak of height 1000 A.U. in intensity dominates the M^2_X (labeled generically as M^2_{PARL}) Bragg peak of 30 (in directly comparable units). This indicates that the sample is almost saturated M^2_X has the same periodic spacing as N^2. Additionally, M^2_Y and M^2_Z (labeled generically as M^2_{PERP}) are small, but not negligible. In fact, they can be modeled as a canted shell 1 nm thick [13] with some uniform magnetic component oriented perpendicular to the applied field per particle. This magnetic core-canted shell morphology can be made to disappear by reducing the applied field to 0.005 Tesla at 300 K [13] (not shown).

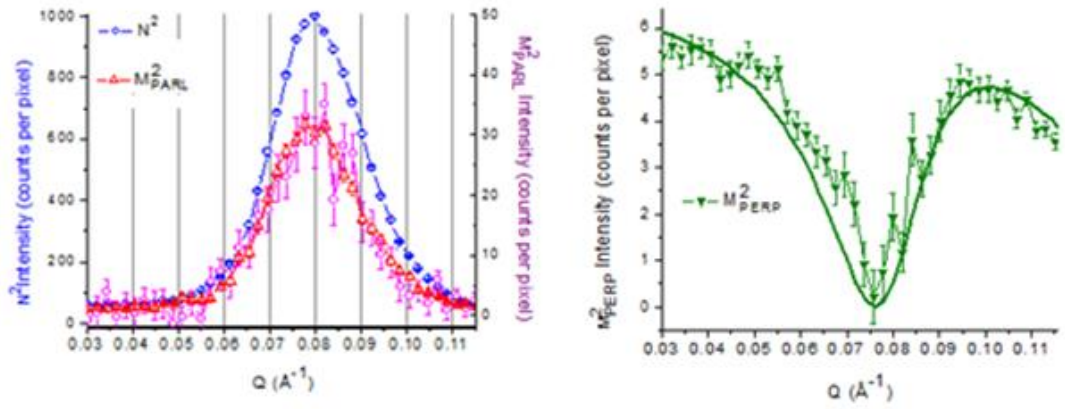

Figure 9. Applying the sector cuts, shown in Figure 8, result in the separation of nuclear scattering, magnetic moments along X || H (M^2_{PARL}), and magnetic moments along Y or Z $\perp$ H (M^2_{PERP}). The Bragg peak does not show up in the perpendicular scattering because these magnetic structures are only correlated over a few nanoparticles, rather than being correlated across each much longer-ranged, face-centered cubic crystal.

6. Data Collection

Let us return the experiment at hand: $CoFe_2O_4$ close-packed nanoparticles. In order to properly reduce your data you will need to collect several types of data files. Transmissions are collected with the beamstop removed (translated to the side) in order to survey the unscattered neutron

beam; these are taken with a series of attenuating filters to insure this main neutron beam isn't so intense so as to burn the detector. Scattering files, on the other hand, make use of a beamstop that blocks this main beam in order to emphasize the weaker sample scattering observed at higher angles. In this case, a sufficiently large beamstop (1" to 4" possible depending on detector distance and beam collimation) is chosen so that attenuating filters are typically not required. Note that a transmission file will be used to define the beam center (from which Q is calculated), while a scattering file will be used to align the beamstop with respect to the main beam.

6.1 Normalization of scattering intensity onto an absolute scale

You will collect transmissions (all at the same attenuation and detector distance) for the sample in a sample holder (a sealed Al can), the sample holder by itself, and an open beam (no sample or sample holder). You will also need a blocked beam in order to account for dark current detector noise. These will provide absolute scale normalization.

6.2 Unpolarized transmissions through the ^{3}He analyzer

The ^{3}He spin filter (analyzer) is pre-pumped into a polarized state with optical pumping, but decays over time with a half-life on the order of 80 – 200 hours. In order to measure the effective polarization of this filter and the reduction in transmission of the preferred spin state over time, you will need to measure a series of *unpolarized* (*i.e*. supermirror moved out of the beam) transmissions through the ^{3}He filter. Precisely, this includes a series of open beam transmissions (^{3}He translated out of the beam), ^{3}He transmission (^{3}He translated into the beam), and a blocked beam transmission – all taken for the same counting time (180 seconds), at the same detector distance and with the same number of attenuators.

6.3 Polarized transmissions to correct for supermirror and flipper polarization efficiency

Using a combination of supermirror, flipper, and 3He spin filter four transmission measurements made be made (↑↑, ↓↑, ↓↓, and ↑↓). The assumptions are that in transmission, rather than sample scattering, (1) any spin-flip is due to beam depolarization and (2) the non-spin flip cross-sections are equal in intensity. From this, you will be able to calculate the polarization of the flipper, as well as the beam/sample depolarization times the polarization of the supermirror.

6.4 Polarized scattering files (sample in holder and sample holder alone "background")

File Header	Purpose	SM State	Flipper State	Sample Position	3He State	Trans or Scatt	Typical Time (seconds)

A.	Abs. Scale	In	Off	OPEN	Out	T	180
B.	Normalize	Out	Off	OPEN	Out	T	180
C.	Normalize	Out	Off	SAMPLE	Out	T	180
D.	Normalize	Out	Off	BLOCK	Out	T	180
E.	3He Pol.	Out	Off	SAMPLE	Out	T	180
F.	3He Pol.	Out	Off	SAMPLE	In	T	180
G.	3He Pol.	Out	Off	BLOCK	Out	T	180
H.	SM,F Pol.	In	OFF	SAMPLE	In, UP	T	180
I.	SM,F Pol.	In	ON	SAMPLE	In, UP	T	180
J.	SM,F Pol.	In	ON	SAMPLE	In, DOWN	T	180
K.	SM,F Pol.	In	OFF	SAMPLE	In, DOWN	T	180
L.	SM,F Pol.	In	OFF	BLOCK	OUT	T	180
M.	Data	IN	OFF	SAMPLE	IN, UP	S	3600
N.	Data	IN	ON	SAMPLE	IN, UP	S	3600
O.	Data	IN	ON	SAMPLE	IN, DOWN	S	3600
P.	Data	IN	OFF	SAMPLE	IN, DOWN	S	3600
Q.	BKGD Data	IN	OFF	BLOCK	OUT	S	300

Table II. Summary of the transmission/scattering files needed to properly reduce and scale PASANS data. Some apparent redundancy is included as a reminder that each grouping of measurements must be taken under the same conditions (same sample, same number of attenuators, etc.)

7 Data Reduction

As a starting point the $CoFe_2O_4$ nanoparticles will be examined at 200 K, 1.2 Tesla in order to most directly compare the results to the Fe_3O_4 nanoparticle system described in this write-up. If time permits, you may choose a second condition (field, temperature, or detector distance) to run overnight. Your instructors will show you how to properly reduce your data within the SANS IGOR framework [20]. Specifically, you will be using the polarized beam module. Additional information about the ^{3}He time dependence and polarization corrections can be found at [21]. In summary, using the provided software you will (1) determine the time dependence of the ^{3}He filter polarization, (2) determine the efficiency of the supermirror, flipper and any depolarization caused by the sample itself (often the result of internal magnetic domains), (3) polarization correct your scattering files based on the information in steps 1 and 2, and (4) background subtract and normalize your scattering data (four cross sections in total) onto absolute scale. In the end you will have four, absolute-scaled cross-sections (↑↑, ↓↑, ↓↓, and ↑↓) of scattering data per sample to work with.

8 Data Analysis

Using the angular cuts discussed in Section 5, you will transform your reduced scattering data (Section 6) into nuclear and magnetic scattering contributions. From here, the SASVIEW Analysis package [22] will be used to model these scattering profiles, including factors such as smearing from wavelength spread, collimation, and sample polydispersity. In particular, you will

be heavily using the core-shell model, face-centered cubic (FCC) paracrystal model, and the body-centered cubic (BCC) paracrystal model. More information about these models can be found at [20]. Your instructors will work with you to model your data and extract key information regarding the nuclear (structural) and magnetic morphology.

Specifically, you should be able to answer the following questions regarding the 9-10 nm $CoFe_2O_4$ close-packed nanoparticle system:

- Does the FCC or BCC paracrystal model work better to fit the structural scattering? What is the average spacing between the nanoparticles?
- What is the magnetic to nuclear intensity ratio at 1.2 Tesla? How does this compare with bulk $CoFe_2O_4$ as given in Table I. (i.e. how much magnetization reduction is seen in the nanoparticle form)?
- How much of the sample magnetization has a component that does not lie along the applied magnetic field?
- What form factor best fits the $M^{\perp} H$ component: a core-shell model like the one observed for the Fe_3O_4 nanoparticles, a model in which the surface spins are disordered, or something else entirely?
- Given that the $CoFe_2O_4$ nanoparticles have nearly the same magnetization density, size, and packing as the example Fe_3O_4 nanoparticle system, but differ primarily in their internal magnetic anisotropy, how similar/dissimilar are the magnetic morphologies of these systems? Does this make sense?
- If a second field/temperature/detector distance is chosen, what does this tell you about the system? Is the net magnetization (considering both $M^2_{||}$ and $M^2_{\perp}$) conserved or does it change? Do the magnetic correlations between the nanoparticles vary?

[1] P. Dutta et al., J. Appl. Phys. 105, 07B501 (2009).

[2] J. Curiale et al., Appl. Phys. Lett. 95, 043106 (2009).

[3] A. Kovacs et al., Phys. Rev. Lett. 103, 115703 (2009).

[4] C. Westman et al., J. Phys. D 41, 225003 (2008).

[5] R. Yanes et al., Phys. Rev. B 76, 064416 (2007).

[6] J. Mazo-Zuluaga, J. Restrepo, and J. Maria-López, Physica (Amsterdam) 398B, 187 (2007).

[7] J. Mazo-Zuluaga et al., J. Appl. Phys. 105, 123907 (2009).

[8] L. Berger et al., Phys. Rev. B 77, 104431 (2008).

[9] Y. Hu A and Du, J. Nanosci. Nanotechnol. 9, 5829 (2009).

[10] J. Salafrana et al., Nano Lett 12, 2499-2503 (2012)

[11] M. Darbundi et al., J. Phys. D: Appl. Phys. 45, 195001 (2012).

[12] A. G. Roca et al., J. Appl. Phys. 105, 114309 (2009)

[13] K.L. Krycka et al., Phys. Rev. Lett. 104, 207203 (2010)

[14] V.F. Sears, Neutron News 3, 29-37 (1992)

[15] http://sld-calculator.appspot.com/

[16] S.R. Ahmed et al., Appl. Phys. Lett. 80, 1616 (2002)

[17] R.M. Moon, T. Riste, and W.C. Koehler Phys. Rev. 181, 920 (1969)

[18] Michels, A. & Weissmu¨ ller, J. (2008). Rep. Prog. Phys. 71, 066501.

[19] K.L. Krycka et al., J. Appl. Cryst. 45, 554 (2012)

[20] ftp://ftp.ncnr.nist.gov/pub/sans/kline/Download/SANS_Model_Docs_v4.10.pdf; S. R. Kline, J Appl. Cryst. 39(6), 895 (2006); http://www.ncnr.nist.gov/programs/sans/data/red_anal.html

[21] K.L. Krycka et al., J. Appl. Cryst. 45, 546 (2012)

[22] http://www.sasview.org/